Transient probe spectra in strongly driven atoms and their dependence on initial atomic conditions

Ning Lu and P. R. Berman
Physics Department, New York University, 4 Washington Place, New York, New York 10003

A. G. Yodh, Y. S. Bai, and T. W. Mossberg
Department of Physics, Harvard University, Cambridge, Massachusetts 02138
(Received 10 October 1985)

We analyze the transient probe spectra that arise when a three-level atom is strongly driven by an optical field nearly resonant with one transition and is probed by a step-function weak field on a coupled transition. We pay particular attention to the effect of imbalances in the initial dressed-state populations on the observed spectra. As recently pointed out, such imbalances may be induced by sudden changes in the *phase* of the driving field. We find that transient probe spectra may differ dramatically for different initial atomic conditions. We follow the temporal relaxation of these novel probe spectra to their steady-state form. Our calculations do not include the effect of inhomogeneous broadening and are hence appropriate to studies of collimated atomic beams.

I. INTRODUCTION

Atomic fluorescence or absorption spectra can be significantly modified in the presence of a strong optical field. In particular, it is now well known[1] that the fluorescence spectrum emitted by a "two-level" atom which is driven by a strong, nearly resonant, cw optical field is split into three spectral components. In addition to modifications in the fluorescence spectrum, one can also observe changes in the absorption or emission spectra of a weak "probe" field that interacts with atoms being driven by a strong "pump" field. Thus, probe absorption spectra can consist of an absorption-emission doublet[2] when the probe and pump fields drive the same atomic transition or an absorption (or emission) doublet[3] when the probe field drives a transition sharing one common level with the pump transition. All the above effects can be explained in a unified manner by using a "dressed-atom" description of the atom-field interaction.[4] In the dressed-atom approach, eigenstates of the atom plus pump field serve as the basis states for the system. The various spectral components observed in fluorescence or absorption are viewed as arising from transitions between these dressed states. Although the radiation field is quantized in the conventional dressed-atom approach,[4] for most applications it is possible to introduce semiclassical dressed states[5,6] in which the optical fields are treated classically.

The doublets and triplets in the pump-modified fluorescence and absorption spectra are features which are found in a "steady-state" limit; that is, all transient effects related to the turn on of the pump and/or probe fields are assumed to have decayed away when the spectra are measured. Although one is often concerned only with the steady-state spectra, there can be interesting information available in the transient regime. In this paper we use a semiclassical dressed-atom approach to calculate what may be termed "transient probe spectra." We are particularly interested in transient probe spectra that are produced in the following manner: (1) a step-function pump field is applied to the atomic sample; (2) at some time ($t=0$) following the application of this field, its phase is switched to produce some desired population of dressed states;[7] (3) at the same time ($t=0$), a step-function probe field is applied to the sample; (4) the transient probe spectrum is monitored for $t \geq 0$. The use of a phase-controlled driving field to control dressed-state populations has recently been demonstrated.[7] With the ability to control the initial dressed-state populations, one can expect to see new and novel features (e.g., suppression of some of the spectral components) in the transient probe spectra.

Using the dressed-atom approach, one can calculate transient probe spectra for the three classes of problems described above (fluorescence spectrum for a driven two-level atom, probe absorption in a driven two-level atom, probe absorption on a transition coupled to the pump transition). In this paper, we restrict the calculation to the pump-probe scheme shown in Fig. 1(a) in which the pump and probe fields act on transitions sharing but one common level. All effects of Doppler broadening are neglected so that our calculations are appropriate to investigations involving collimated atomic beams. Transient probe-absorption spectra are obtained for arbitrary initial conditions for the dressed states of the system. Related calculations have appeared involving transients in three-level systems,[5,6,8–20] the time dependence of resonance fluorescence spectra,[18,21] quantum beats from dressed atoms,[19] photon echoes from dressed atoms,[20] transient effects in probe-absorption spectra resulting from optical pumping,[22] and the transient probe field spectrum observed when a cw pump is suddenly turned *off*.[23] It may be noted that transient resonance fluorescence line shape was studied as a function of initial atomic conditions by Eberly *et al.*[21] However, these calculations are not specifically oriented towards studying the transient probe spectra as a function of the initial *dressed-state* amplitudes.

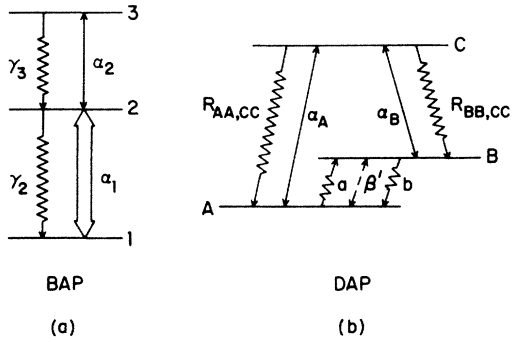

FIG. 1. Upward-cascade three-level closed system in both (a) bare-atom picture (BAP) and (b) the dressed-atom picture (DAP). (a) In the BAP, levels 1 and 2 are coupled by a strong field α_1 ($=|\chi|/2$) and levels 2 and 3 by a weak probe field α_2. Level 3 decays back to level 2 and level 2 decays back to level 1. (b) In the DAP, the dressed states are coupled by α_A and α_B (which are proportional to the probe field strength) and a, b, β', $R_{AA,CC}$, and $R_{BB,CC}$ (which are proportional to the decay rates). The levels for the DAP are drawn in an interaction representation in which the laser photon energies have been subtracted out.

As such, they miss many of the novel features that appear when the atoms are prepared in specific arrangements of the dressed states.

In Sec. II, we give a qualitative discussion of the problem addressed herein. A detailed calculation of transient probe spectra is presented in Sec. III, and the dependence of the spectrum on the initial atomic conditions is discussed for various special cases in Sec. IV. Finally, in Sec. V, we discuss dressed-atom state preparation.

II. QUALITATIVE DISCUSSION OF TRANSIENT PROBE SPECTROSCOPY IN A THREE-LEVEL SYSTEM

The response of a two-level system driven by a nearly resonant field is often described by the Bloch equation,[24] which may be written (neglecting relaxation) as

$$\frac{d\mathbf{B}}{dt}=\mathbf{\Omega}_B\times\mathbf{B}\ , \tag{2.1}$$

where $\mathbf{\Omega}_B=(-\chi,0,\Delta_{21})$ is the driving field vector and $\mathbf{B}=(u,v,w)$ is the Bloch vector. The quantity $\chi=\mathbf{p}_{21}\cdot\mathscr{E}_1/\hbar$ is the Rabi frequency associated with a driving field of the form $\mathscr{E}_1\cos(\Omega_1 t-\mathbf{K}_1\cdot\mathbf{r}+\phi_1)$ and has been chosen to be real,[25] Δ_{21} is the atom-field detuning, $\mathbf{p}_{21}$ is an atomic dipole-moment matrix element, and u, v, and w are related to atomic density-matrix elements $\tilde{\rho}_{ij}$ in the field-interaction representation[6,25] by

$$\begin{aligned} u&=\tilde{\rho}_{12}+\tilde{\rho}_{21}\ ,\\ v&=i(\tilde{\rho}_{21}-\tilde{\rho}_{12})\ ,\\ w&=\tilde{\rho}_{22}-\tilde{\rho}_{11}\ ,\\ \tilde{\rho}_{11}&+\tilde{\rho}_{22}=1\ . \end{aligned} \tag{2.2}$$

The fact that the Bloch vector lies in the uw plane is linked to our (conventional) definition of the interaction representation.[25] If an additional phase angle $-\delta$ is introduced into the definition of the interaction representation, the Bloch vector has components $(-\chi\cos\delta,-\chi\sin\delta,\Delta_{21})$. It is clear from Eq. (2.1) that the temporal evolution of $\mathbf{B}$ can be quite different depending on its orientation relative to $\mathbf{\Omega}_B$. In general, $\mathbf{B}$ precesses about $\mathbf{\Omega}_B$ in such a way that the relative angle between the two vectors remains fixed, i.e., $\mathbf{B}$ precesses in a cone about $\mathbf{\Omega}_B$. The extent of the Bloch vector's motion is clearly largest when $\mathbf{\Omega}_B$ and $\mathbf{B}$ are orthogonal and minimum (in fact $\mathbf{B}$ remains stationary) when $\mathbf{B}$ and $\mathbf{\Omega}_B$ are parallel or antiparallel. Interestingly, it has recently been pointed out that the configurations with $\mathbf{B}\|(\pm\mathbf{\Omega}_B)$ correspond to atoms in particular dressed states of the atom-field system.[5,7] Since the u and v components of $\mathbf{B}$ are related to the electric dipole moment of the atom, their oscillation or nonoscillation should be reflected in the spectra of the driven atom.

In steady-state strong-field spectra measurements, one essentially averages over the behavior of atoms with many different relative orientations between $\mathbf{B}$ and $\mathbf{\Omega}_B$. However, as was recently demonstrated experimentally,[7] it is possible, in the transient case, to excite a sample of atoms so that the Bloch vectors of all atoms have a particular orientation with respect to the driving field. In particular, the special case in which the Bloch vector of all the atoms are aligned parallel to $\pm\mathbf{\Omega}_B$ (i.e., when all the atoms are excited into a particular dressed state) has been shown to be experimentally accessible. The means of exciting atoms into a particular dressed state is analogous to that employed in the "spin-locking" experiments of nuclear magnetic resonance[26] and will be discussed further in Sec. V. Although the Bloch vector picture does not provide immediate intuitive insight into the problem of atoms interacting with both a pump and a probe field, we can expect that the initial relative orientation of $\mathbf{B}$ and $\mathbf{\Omega}_B$ will have a strong influence on the transient probe spectra.

In this paper we are concerned with understanding the spectral response of the probe absorption signal in a single velocity subclass of three-level atoms shown in Fig. 1(a). We assume that in the time period before $t=0$ the atoms are prepared (in a manner to be discussed in Sec. V) such that a given set of initial conditions for the components of the Bloch vector $\mathbf{B}_{12}$ associated with the 1-2 transition or, equivalently, for density-matrix elements $[\tilde{\rho}_{12}(t=0)$, $\tilde{\rho}_{21}(t=0)$, $\tilde{\rho}_{22}(t=0)]$, is achieved. For $t>0$, a strong cw pump field with associated Rabi frequency χ drives only the 1-2 transition while a weak probe field is used to study the spectrum associated with the 2-3 transition. The probe absorption is then monitored as a function of time, probe-field—atom detuning Δ_{32}, and the initial conditions of the Bloch vector. For a strong *resonant* pump field, the *steady-state* probe absorption as a function of Δ_{32} is shown in Fig. 2, where the separation of the two peaks corresponds to the well-known ac Stark splitting.[3] Our problem then is to trace the time evolution of the probe absorption from $t=0$ to this steady-state distribution.

Since the pump laser field coupling the 1-2 transition is intense, a dressed-atom picture (DAP) provides a good approach for studying the problem.[4–6] Usually in the DAP, all or part of the atom-field interaction is solved exactly and the resultant atom-field eigenstates are used as the

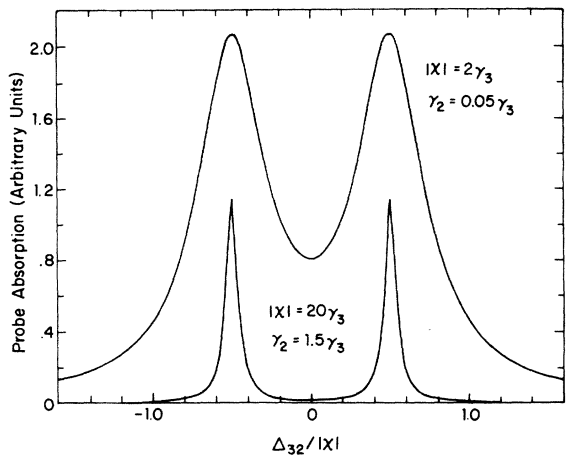

FIG. 2. Steady-state probe absorption as a function of dimensionless probe detuning $\Delta_{32}/|\chi|$ when a strong pump field is exactly on resonance with the 1-2 transition. These curves also give the steady-state value of the upper level population $\tilde{\rho}_{33}(t\sim\infty)$ as a function of $\Delta_{32}/|\chi|$. The two curves shown correspond to different ratios of the Rabi frequency χ and decay rate γ_2 to the decay rate γ_3.

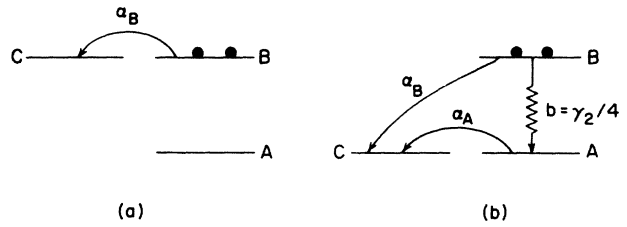

FIG. 3. Energy levels of the three-level system with a strong resonant dressing field and $\tilde{\rho}_{BB}(0)=1$ in the DAP when the probe is resonant with (a) initially populated state B ($\omega_{CB}=0$) and (b) initially unpopulated state A ($\omega_{CA}=0$). In (a), the probe absorption builds up proportional to t initially and reaches its steady-state value with no oscillation. In (b), except for a small oscillatory component arising from a nonresonant direct coupling between levels B and C, the probe absorption builds up, on average, proportional to t^2 initially via the level coupling $B\rightarrow A\rightarrow C$. The probe absorption in (a) ($\omega_{CB}=0$) is much larger than that in (b) ($\omega_{CA}=0$) at early times. In this figure, α_A and α_B give the probe coupling strengths, while b is the rate of transfer of population from state B to A.

basis for further calculations. Here, the strong pump field can be viewed as a dressing field for an atom. It produces the semiclassical dressed states $|A\rangle$, $|B\rangle$, and $|C\rangle$ [see Fig. 1(b)] in which the states $|A\rangle$ and $|B\rangle$ are a linear combination of the bare-atom picture (BAP) basis vectors $|\tilde{1}\rangle$ and $|\tilde{2}\rangle$ and state $|C\rangle$ corresponds to state $|\tilde{3}\rangle$, with all the energies modified to account for the fact that we use a field-interaction representation.[6,27]

The two peaks appearing in the steady-state spectrum are easily explained in terms of the DAP. For a fixed pump field detuning Δ_{21}, states A and B are separated in frequency by $\omega_{BA}=(\Delta_{21}^2+\chi^2)^{1/2}$.[6] As the probe field detuning Δ_{32} is varied, level C moves vertically since $\omega_C=\Delta_{32}$;[27] resonances occur when level C becomes degenerate with either level A or B. As such, the probe-absorption spectrum consists of two peaks separated in frequency by ω_{BA}.

We are now in a position to understand qualitatively the effect of initial conditions on the transient probe spectrum. For simplicity, we consider the case of a resonant dressing field only ($\Delta_{21}=0$, $\omega_{BA}=|\chi|$) and the limit when the Rabi frequency χ is much larger than all relaxation rates (the more general case is considered in Sec. III). We consider the probe spectrum resulting from two different sets of initial atomic conditions at $t=0$. In the first, the atoms are assumed prepared in the B dressed state, i.e., $\tilde{\rho}_{BB}(t=0)=1$, $\tilde{\rho}_{AA}(0)=0$. In the second, the atoms are assumed to reside in "bare" state $|\tilde{1}\rangle$ [i.e., $\tilde{\rho}_{11}(0)=1$] which implies that $\tilde{\rho}_{AA}(0)=\tilde{\rho}_{BB}(0)=\tilde{\rho}_{AB}(0)=\tilde{\rho}_{BA}(0)=\frac{1}{2}$.

Case 1: $\tilde{\rho}_{BB}(0)=1$. For a probe detuning $\Delta_{32}=|\chi|/2$, the probe is resonant with the initially populated dressed state B (Fig. 3). This leads to a relatively large probe absorption with no oscillatory behavior owing to the resonance between dressed states $|B\rangle$ and $|C\rangle$. The probe absorption builds up to its steady-state value with no oscillation. For a probe detuning $\Delta_{32}=-|\chi|/2$, state C is resonant with the (initially unpopulated) dressed state A. Probe absorption occurs via two pathways. First, there is direct coupling between states B and C. Since this is off-resonance coupling, it leads to oscillation in the probe absorption buildup when the probe field is detuned at $\Delta_{32}=-|\chi|/2$. However, the relatively large oscillation frequency (large relative to relaxation rates) usually results in a relatively small contribution to this component of the probe absorption. The second pathway involves a coupling of level B to A (this coupling occurs at a rate comparable to the spontaneous decay rate of level 2) and a subsequent resonant coupling of level A to level C. This contribution is nonoscillatory. At early times state A's population is much less than that of state B, implying that the probe absorption is greater for $\Delta_{32}=|\chi|/2$ than for $\Delta_{32}=-|\chi|/2$. As $t\rightarrow+\infty$, both $\tilde{\rho}_{AA}$ and $\tilde{\rho}_{BB}$ approach their equilibrium values of $\frac{1}{2}$ and the absorption spectrum achieves its steady-state form with equal absorption for $\Delta_{32}=\pm|\chi|/2$. Thus for the $\tilde{\rho}_{BB}(0)=1$ initial condition there is minimal oscillation in the probe absorption signal, and the probe absorption at $\Delta_{32}=|\chi|/2$ is initially stronger than that for $\Delta_{32}=-|\chi|/2$. The absence of strong oscillation in the probe absorption versus time is linked to the fact that the Bloch vector $\mathbf{B}_{12}$ and the $\mathbf{\Omega}_B$ vector are initially aligned at $t=0$.

Case 2: $\tilde{\rho}_{11}(0)=1$, i.e., $\tilde{\rho}_{AA}^{(0)}=\tilde{\rho}_{BB}^{(0)}=\tilde{\rho}_{AB}^{(0)}=\tilde{\rho}_{BA}^{(0)}=\frac{1}{2}$. In this limit, there is still the nonoscillatory contribution to the probe absorption for each of the probe detunings $\Delta_{32}=\pm\chi/2$ discussed above (these contributions are now the *same* for $\Delta_{32}=\chi/2$ and $\Delta_{32}=-\chi/2$ owing to the inherent symmetry in the initial conditions). However, there is an additional major contribution to the probe absorption which comes from the fact that $\tilde{\rho}_{BA}\neq0$ at $t=0$. This dressed-state coherence also leads to probe absorption at $\Delta_{32}=\pm\chi/2$ but this contribution oscillates in time at a frequency equal to $|\chi|$. In the Bloch picture this corresponds to the fact that the Bloch vector $\mathbf{B}_{12}$ is not initially aligned along the $\mathbf{\Omega}_B$ vector—precession of the

Bloch vector translates into an oscillatory probe-absorption signal.

In closing this section, we briefly comment on the time-frequency uncertainty relation and its role in the measurement of the transient spectra calculated here. In previous discussions related to transient resonant fluorescence,[21,28] it has been pointed out that the need to simultaneously measure the spectral and temporal properties of light observed in transient spectra leads to unavoidable limits on the achievable temporal resolution. The probe spectra calculated here, however, are unaffected by the temporal-spectral uncertainty relation for the simple reason that the temporal and spectral measurements are not made simultaneously. No spectral filtering need be performed on the signals observed during the actual transient experiment. The probe frequency, corresponding to a cw laser frequency, is determined at one's convenience before or after the transient measurement. Thus, as long as one has detectors that are sufficiently fast to record the probe absorption as a function of time for a given probe frequency, there is no problem, analogous to the one encountered in measuring the fluorescence spectrum as a function of time, in defining what is the physically observed variable. The problem of a time-dependent fluorescence spectrum for atoms prepared in pure dressed states will be discussed in a future paper.

III. PHYSICAL SYSTEM AND SOLUTION

Consider an atomic beam traveling in the x direction which interacts with a composite optical field of the form

$$\mathbf{E}(y,z,t)=\mathscr{E}_1\cos(\Omega_1 t-\mathbf{K}_1\cdot\mathbf{r}+\phi_1)+\mathscr{E}_2\cos(\Omega_2 t-\mathbf{K}_2\cdot\mathbf{r}+\phi_2)\ , \tag{3.1}$$

with $K_{1x}=K_{2x}=0$. The atoms are modeled as having three levels, 1, 2, and 3, with energy difference $\hbar\omega_{ij}$ between levels i and j. The laser field $(\mathscr{E}_1,\Omega_1)$ is a strong pump field and effectively drives the 1-2 transition only, while the laser field $(\mathscr{E}_2,\Omega_2)$ is a weak probe field which effectively drives the 2-3 transition only. Owing to the use of the atomic beam with $\mathbf{K}_1\cdot\mathbf{v}=\mathbf{K}_2\cdot\mathbf{v}=0$ ($\mathbf{v}$ is the velocity of the atomic beam), contributions to atom-field detunings arising from the linear Doppler effect are eliminated. In the following calculation, we will follow the notation in the paper of Berman and Salomaa,[6] and make use of the results obtained therein.

We want to find the transient behavior of the probe to lowest order in $|\mathscr{E}_2|$. The laser field $(\mathscr{E}_1,\Omega_1)$ can be viewed as a dressing field for the atom, producing the semiclassical dressed states (using a field-interaction representation[6,25,27])

$$\begin{aligned}|A\rangle&=\cos\theta|\tilde{1}\rangle-\sin\theta|\tilde{2}\rangle\ ,\\ |B\rangle&=\sin\theta|\tilde{1}\rangle+\cos\theta|\tilde{2}\rangle\ ,\\ |C\rangle&=|\tilde{3}\rangle\ ,\end{aligned} \tag{3.2}$$

where

$$\sin\theta=\{\tfrac{1}{2}[1-\Delta_{21}(\Delta_{21}^2+4\alpha_1^2)^{-1/2}]\}^{1/2}\ , \tag{3.3}$$

$$\alpha_1=-\chi/2=-\mathbf{p}_{21}\cdot\mathscr{E}_1/2\hbar\ , \tag{3.4}$$

$$\Delta_{21}=\omega_{21}-\mathrm{sgn}(\omega_{21})\Omega_1\ , \tag{3.5}$$

α_1 has been chosen to be real and positive, and θ is defined such that $0\le\theta\le\pi/2$. The frequency separation of the dressed states is

$$\omega_{CA}=\Delta_{32}+\tfrac{1}{2}\Delta_{21}+\tfrac{1}{2}(\Delta_{21}^2+4\alpha_1^2)^{1/2}\ , \tag{3.6a}$$

$$\omega_{CB}=\Delta_{32}+\tfrac{1}{2}\Delta_{21}-\tfrac{1}{2}(\Delta_{21}^2+4\alpha_1^2)^{1/2}\ , \tag{3.6b}$$

$$\omega_{BA}=(\Delta_{21}^2+4\alpha_1^2)^{1/2}\ , \tag{3.6c}$$

where

$$\Delta_{32}=\omega_{32}-\mathrm{sgn}(\omega_{32})\Omega_2\ .$$

For the DAP picture to be useful, we require that ω_{BA} be much greater than all relaxation rates associated with levels 1 and 2.

Assuming that relaxation processes in the BAP (see Ref. 6) can be modeled by

$$(\dot{\tilde{\rho}}_{\mathrm{rel}})_{ij}=-\gamma_{ij}\tilde{\rho}_{ij}\quad(i\neq j)\ , \tag{3.7a}$$

$$(\dot{\tilde{\rho}}_{\mathrm{rel}})_{ii}=-\Gamma_i\tilde{\rho}_{ii}+\sum_{j\,(\neq i)}\Gamma_{ji}\tilde{\rho}_{jj}\ , \tag{3.7b}$$

with $\Gamma_{31}=\Gamma_{13}=0$, and that incoherent pumping of the bare states is governed by the rates

$$\Lambda_{ij}=\Lambda_i\delta_{ij}\ , \tag{3.8}$$

the equations of the density-matrix elements in the DAP are

$$\dot{\tilde{\rho}}_{AA}=\Lambda_A+R_{AA,\mu\nu}\tilde{\rho}_{\mu\nu}+2\alpha_A\,\mathrm{Im}(\tilde{\rho}_{CA})\ , \tag{3.9a}$$

$$\dot{\tilde{\rho}}_{BB}=\Lambda_B+R_{BB,\mu\nu}\tilde{\rho}_{\mu\nu}+2\alpha_B\,\mathrm{Im}(\tilde{\rho}_{CB})\ , \tag{3.9b}$$

$$\dot{\tilde{\rho}}_{CC}=\Lambda_C+R_{CC,\mu\nu}\tilde{\rho}_{\mu\nu}-2\alpha_A\,\mathrm{Im}(\tilde{\rho}_{CA})-2\alpha_B\,\mathrm{Im}(\tilde{\rho}_{CB})\ , \tag{3.9c}$$

$$\dot{\tilde{\rho}}_{CA}=-(\gamma_{CA}+i\omega_{CA})\tilde{\rho}_{CA}+i\alpha_A(\tilde{\rho}_{CC}-\tilde{\rho}_{AA})-i\alpha_B\tilde{\rho}_{BA}+\beta'\tilde{\rho}_{CB}\ , \tag{3.9d}$$

$$\dot{\tilde{\rho}}_{CB}=-(\gamma_{CB}+i\omega_{CB})\tilde{\rho}_{CB}+i\alpha_B(\tilde{\rho}_{CC}-\tilde{\rho}_{BB})-i\alpha_A\tilde{\rho}_{AB}+\beta'\tilde{\rho}_{CA}\ , \tag{3.9e}$$

$$\dot{\tilde{\rho}}_{BA}=\Lambda_{BA}+R_{BA,\mu\nu}\tilde{\rho}_{\mu\nu}-(\gamma_{BA}+i\omega_{BA})\tilde{\rho}_{BA}+i\alpha_A\tilde{\rho}_{BC}-i\alpha_B\tilde{\rho}_{CA}\ , \tag{3.9f}$$

$$\tilde{\rho}_{\mu\nu}=\tilde{\rho}^*_{\nu\mu}\ , \tag{3.9g}$$

where

$$\Lambda_A=\Lambda_1\cos^2\theta+\Lambda_2\sin^2\theta\ , \tag{3.10a}$$

$$\Lambda_B=\Lambda_1\sin^2\theta+\Lambda_2\cos^2\theta\ , \tag{3.10b}$$

$$\Lambda_C=\Lambda_3\ , \tag{3.10c}$$

$$\Lambda_{BA}=\Lambda_{AB}=\tfrac{1}{2}(\Lambda_1-\Lambda_2)\sin^2\theta\ , \tag{3.10d}$$

$$\alpha_A=-\alpha_2\sin\theta\ , \tag{3.11a}$$

$$\alpha_B=\alpha_2\cos\theta\ , \tag{3.11b}$$

$$\alpha_2=-\mathbf{p}_{32}\cdot\mathscr{E}_2/2\hbar\ , \tag{3.11c}$$

$$\beta'=\tfrac{1}{2}(\gamma_{32}-\gamma_{31})\sin(2\theta)\ , \tag{3.12a}$$

$$\gamma_{CA}=\gamma_{31}\cos^2\theta+\gamma_{32}\sin^2\theta\ , \tag{312b}$$

$$\gamma_{CB}=\gamma_{31}\sin^2\theta+\gamma_{32}\cos^2\theta\ , \tag{3.12c}$$

$$\gamma_{BA}=\gamma_{21}+\tfrac{1}{4}(\Gamma_{12}+\Gamma_{21}-\eta)\sin^2(2\theta)\ , \tag{3.12d}$$

$$\eta=2\gamma_{21}-\Gamma_1-\Gamma_2\ , \tag{3.13}$$

and the summation convention is implied in Eqs. (3.9). The quantity η gives a measure of the effect of phase-changing collisions ($\eta=0$ in the absence of collisions), α_2 has been chosen to be real, and the nonvanishing $R_{\xi\sigma,\mu\nu}$ are given in Appendix A. The γ_{ij} $(i,j=1,2,3,\ i\neq j)$ are decay rates associated with the $\tilde{\rho}_{ij}$ coherence.

The physical observables are the probe-absorption coefficient which is proportional to $\mathrm{Im}(\tilde{\rho}_{32})$ with

$$\tilde{\rho}_{32}=\cos\theta\,\tilde{\rho}_{CB}-\sin\theta\,\tilde{\rho}_{CA}\ , \tag{3.14}$$

and the population of level 3

$$\tilde{\rho}_{33}=\tilde{\rho}_{CC}\ . \tag{3.15}$$

The population $\tilde{\rho}_{33}(t)$ is a measure of the instantaneous spectrally integrated fluorescence from level 3 that one would observe if the probe field is abruptly turned off at time $t>0$. Equations (3.9) are to be solved to lowest order in α_2, which implies that we must find $\tilde{\rho}_{CA}$ and $\tilde{\rho}_{CB}$ to first order in α_A or α_B and $\tilde{\rho}_{CC}$ to second order in these quantities. For algebraic simplicity, we consider here a specific case—upward cascade for a closed system (see Fig. 1).

The closed system is characterized by incoherent pumping rates

$$\Lambda_i=0\ \ (i=1,2,3)\ , \tag{3.16}$$

and relaxation rates

$$\Gamma_2=\Gamma_{21}=\gamma_2\ , \tag{3.17a}$$

$$\Gamma_3=\Gamma_{32}=\gamma_3\ , \tag{3.17b}$$

$$\Gamma_1=\Gamma_{12}=\Gamma_{23}=0\ . \tag{3.17c}$$

Equations (3.17) imply that all spontaneous emission from level 3 returns to level 2 and that from level 2 returns to level 1. Moreover, collisions can be neglected, owing to the use of an atomic beam,

$$\eta=0\ , \tag{3.18a}$$

$$\gamma_{i1}=\gamma_i/2\ \ (i=2,3)\ , \tag{3.18b}$$

$$\gamma_{32}=\tfrac{1}{2}(\gamma_3+\gamma_2)\ . \tag{3.18c}$$

The total population is conserved,

$$\tilde{\rho}_{AA}+\tilde{\rho}_{BB}+\tilde{\rho}_{CC}=\tilde{\rho}_{11}+\tilde{\rho}_{22}+\tilde{\rho}_{33}=1\ , \tag{3.19}$$

enabling us to eliminate $\tilde{\rho}_{AA}$ from Eqs. (3.9) and, with the use of Eqs. (3.16)–(3.18), reduce Eqs. (3.9) to

$$\dot{\tilde{\rho}}_{BB}=a-(a+b)\tilde{\rho}_{BB}+R_{BB,AB}(\tilde{\rho}_{AB}+\tilde{\rho}_{BA})+(R_{BB,CC}-a)\tilde{\rho}_{CC}+2\alpha_B\,\mathrm{Im}(\tilde{\rho}_{CB})\ , \tag{3.20a}$$

$$\dot{\tilde{\rho}}_{CC}=-\gamma_3\tilde{\rho}_{CC}-2\alpha_A\,\mathrm{Im}(\tilde{\rho}_{CA})-2\alpha_B\,\mathrm{Im}(\tilde{\rho}_{CB})\ , \tag{3.20b}$$

$$\dot{\tilde{\rho}}_{CA}=-i\alpha_A-(\gamma_{CA}+i\omega_{CA})\tilde{\rho}_{CA}+i\alpha_A(\tilde{\rho}_{BB}+2\tilde{\rho}_{CC})-i\alpha_B\tilde{\rho}_{BA}+\beta'\tilde{\rho}_{CB}\ , \tag{3.20c}$$

$$\dot{\tilde{\rho}}_{CB}=-(\gamma_{CB}+i\omega_{CB})\tilde{\rho}_{CB}+i\alpha_B(\tilde{\rho}_{CC}-\tilde{\rho}_{BB})-i\alpha_A\tilde{\rho}_{AB}+\beta'\tilde{\rho}_{CA}\ , \tag{3.20d}$$

$$\dot{\tilde{\rho}}_{BA}=R_{BA,AA}+(R_{BA,BB}-R_{BA,AA})\tilde{\rho}_{BB}+(R_{BA,CC}-R_{BA,AA})\tilde{\rho}_{CC}-(\gamma_{BA}+i\omega_{BA})\tilde{\rho}_{BA}+i\alpha_A\tilde{\rho}_{BC}-i\alpha_B\tilde{\rho}_{CA}\ , \tag{3.20e}$$

where

$$a=\gamma_2\sin^4\theta\ , \tag{3.21a}$$

$$b=\gamma_2\cos^4\theta\ , \tag{3.21b}$$

and the $R_{\xi\sigma,\mu\nu}$ are given in Appendix A. We consider the case in which field α_1 is constant for $t>0$ and field α_2 is switched on at $t=0$. Since the probe field is "off" for $t<0$, one has initial conditions

$$\tilde{\rho}_{CA}(0)=\tilde{\rho}_{CB}(0)=\tilde{\rho}_{CC}(0)=0\ ,$$
$$\tilde{\rho}_{\mu\nu}(0)\ \text{arbitrary},\ \ \mu,\nu=A\ \text{or}\ B\ . \tag{3.22}$$

Solving Eqs. (3.20c) and (3.20d) for $\tilde{\rho}_{CA}$ and $\tilde{\rho}_{CB}$ to first order in α_A or α_B, we find (assuming $\omega_{BA}\gg\gamma_2$)

$$\dot{\tilde{\rho}}_{CA}=-i\alpha_A-(\gamma_{CA}+i\omega_{CA})\tilde{\rho}_{CA}+i\alpha_A\tilde{\rho}^{(0)}_{BB}-i\alpha_B\tilde{\rho}^{(0)}_{BA}\ , \tag{3.23a}$$

$$\dot{\tilde{\rho}}_{CB}=-(\gamma_{CB}+i\omega_{CB})\tilde{\rho}_{CB}-i\alpha_B\tilde{\rho}^{(0)}_{BB}-i\alpha_A\tilde{\rho}^{(0)}_{AB}\ , \tag{3.23b}$$

where $\tilde{\rho}^{(0)}_{\mu\nu}$ are the zeroth-order solutions for $\tilde{\rho}_{\mu\nu}$ which, to lowest order in γ_2/ω_{BA}, can be easily determined from Eqs. (3.20a) and (3.20e) as

$$\tilde{\rho}^{(0)}_{BB}=e^{-\Gamma_p t}\left[\tilde{\rho}_{BB}(0)-\frac{a}{\Gamma_p}\right]+\frac{a}{\Gamma_p}\ , \tag{3.24a}$$

$$\tilde{\rho}^{(0)}_{BA}=e^{-(\gamma_{BA}+i\omega_{BA})t}\tilde{\rho}_{BA}(0)\ , \tag{3.24b}$$

where

$$\Gamma_p=a+b=\gamma_2(1-\tfrac{1}{2}\sin^2 2\theta)\ . \tag{3.25}$$

Thus, for constant α_2 $(t>0)$, the probe response is determined by

$$\tilde{\rho}_{CA}(t)=-i\left[\alpha_A\frac{e^{-\Gamma_p t}-e^{-(\gamma_{CA}+i\omega_{CA})t}}{\gamma_{CA}+i\omega_{CA}-\Gamma_p}\left[\frac{a\tilde{\rho}_{AA}(0)-b\tilde{\rho}_{BB}(0)}{\Gamma_p}\right]+\alpha_A\left[\frac{b}{\Gamma_p}\right]\frac{1-e^{-(\gamma_{CA}+i\omega_{CA})t}}{\gamma_{CA}+i\omega_{CA}}\right.$$
$$\left.+\alpha_B\tilde{\rho}_{BA}(0)\frac{e^{-(\gamma_{BA}+i\omega_{BA})t}-e^{-(\gamma_{CA}+i\omega_{CA})t}}{i\omega_{CB}+\gamma_{CA}-\gamma_{BA}}\right], \tag{3.26a}$$

$$\tilde{\rho}_{CB}(t)=-i\left[\alpha_B\frac{e^{-\Gamma_p t}-e^{-(\gamma_{CB}+i\omega_{CB})t}}{\gamma_{CB}+i\omega_{CB}-\Gamma_p}\left[\frac{b\tilde{\rho}_{BB}(0)-a\tilde{\rho}_{AA}(0)}{\Gamma_p}\right]+\alpha_B\left[\frac{a}{\Gamma_p}\right]\frac{1-e^{-(\gamma_{CB}+i\omega_{CB})t}}{\gamma_{CB}+i\omega_{CB}}\right.$$
$$\left.+\alpha_A\tilde{\rho}_{AB}(0)\frac{e^{-(\gamma_{BA}-i\omega_{BA})t}-e^{-(\gamma_{CB}+i\omega_{CB})t}}{i\omega_{CA}+\gamma_{CB}-\gamma_{BA}}\right], \tag{3.26b}$$

$$\tilde{\rho}_{32}(t)=\cos\theta\tilde{\rho}_{CB}(t)-\sin\theta\tilde{\rho}_{CA}(t)\ . \tag{3.27}$$

The signal generally consists of both nonoscillatory and oscillatory contributions. As $t\rightarrow+\infty$, it approaches the steady-state behavior shown in Fig. 2.

The level-3 population, second order in α_A or α_B, is found from Eq. (3.20b) to be

$$\tilde{\rho}_{33}(t)=\tilde{\rho}_{CC}(t)=-2\int_0^t e^{-\gamma_3(t-t')}[\alpha_A\mathrm{Im}\tilde{\rho}_{CA}(t')+\alpha_B\mathrm{Im}\tilde{\rho}_{CB}(t')]dt'$$
$$=-2\alpha_2\mathrm{Im}\left[\int_0^t e^{-\gamma_3(t-t')}\tilde{\rho}_{32}(t')dt'\right]. \tag{3.28}$$

By substituting Eqs. (3.27) and (3.26) into Eq. (3.28), one can easily obtain the explicit expression for $\tilde{\rho}_{33}(t)$ which is given in Appendix B.

IV. TRANSIENT SPECTRA—SUPPRESSED PEAKS

Equations (3.26) and (3.27) for the probe absorption [proportional to $\mathrm{Im}\tilde{\rho}_{32}(t)$] and Eq. (3.28) for $\tilde{\rho}_{33}(t)$ are functions of the detunings Δ_{21} and Δ_{32}, the field strength $2\alpha_1=-\chi$, and the time t. For fixed Δ_{21} and χ, one can obtain transient spectra by monitoring the probe absorption or level-3 population (via fluorescence) as a function of Δ_{32} for fixed t. Alternatively, for fixed Δ_{21} and χ, one can observe the transient buildup of the probe absorption as a function of t for fixed Δ_{32}. In this section, we give illustrative examples of both transient spectra and the transient buildup of probe absorption.

Note that, as $t\rightarrow+\infty$, the steady-state value for $\tilde{\rho}_{32}(t)$ from Eq. (3.27) is given by

$$\tilde{\rho}_{32}(\infty)=-i\alpha_2\frac{\sin^2(2\theta)}{4-2\sin^2(2\theta)}\times\left[\frac{\sin^2\theta}{\gamma_{CB}+i\omega_{CB}}+\frac{\cos^2\theta}{\gamma_{CA}+i\omega_{CA}}\right] \tag{4.1}$$

and is *independent* of the initial atomic conditions. The absorption spectrum displays two peaks, at $\omega_{CA}=0$ and $\omega_{CB}=0$. The relative peak amplitudes are a function of Δ_{21}/χ (or θ)—for $\Delta_{21}=0$, the steady-state probe-absorption signal is symmetric about $\Delta_{32}=0$. Except for the inherent difference in peak amplitudes associated with a detuning $\Delta_{21}\neq0$, most of the qualitative features of the transient response do not depend on whether or not $\Delta_{21}=0$. Consequently, we choose to limit our illustrative examples to situations in which $\Delta_{21}=0$ ($\theta=\pi/4$).

The transient probe spectrum given by Eq. (3.26) and (3.27) has a complicated structure even for $\Delta_{21}=0$. In general, at a given time, the spectrum exhibits resonant structure near $\omega_{CA}=\Delta_{32}+\alpha_1=0$ and $\omega_{CB}=\Delta_{32}-\alpha_1=0$, but may oscillate as a function of Δ_{32} between these peaks. For a given Δ_{32}, the buildup of probe absorption in time generally consists of oscillatory and nonoscillatory components. The degree of oscillatory behavior as well as the time it takes for each resonance peak to reach its equilibrium value is a sensitive function of the initial atomic conditions. In order to study this dependence, we first consider the transient buildup of the absorption peaks. Following that discussion, we display transient probe spectra for a number of initial conditions.

A. Transient buildup of absorption peaks

The absorption peaks occur at $\omega_{CB}=0$ and $\omega_{CA}=0$. For $\Delta_{21}=0$ ($\theta=\pi/4$), Eqs. (3.26) and (3.27) may be used to obtain

$$\tilde{\rho}_{32}(t)=-\frac{i\alpha_2}{4}\left[\frac{1-e^{-(\gamma+2i\alpha_1)t}}{\gamma+2i\alpha_1}+\frac{1-e^{-\gamma t}}{\gamma}\right]$$
$$-\frac{i\alpha_2}{4}[\tilde{\rho}_{AA}(0)-\tilde{\rho}_{BB}(0)]\left[\frac{e^{-(1/2)\gamma_2 t}-e^{-(\gamma+i2\alpha_1)t}}{\gamma-\frac{1}{2}\gamma_2+2i\alpha_1}-\frac{e^{-(1/2)\gamma_2 t}-e^{-\gamma t}}{\gamma-\frac{1}{2}\gamma_2}\right]$$
$$+\frac{i\alpha_2}{2}\left[\tilde{\rho}_{BA}(0)\frac{e^{-(3/4)\gamma_2 t}-e^{-\gamma t}}{\gamma-\frac{3}{4}\gamma_2}e^{-i2\alpha_1 t}+\tilde{\rho}_{AB}(0)\frac{e^{-[(3/4)\gamma_2-i2\alpha_1]t}-e^{-\gamma t}}{\gamma-\frac{3}{4}\gamma_2+2i\alpha_1}\right] \quad \text{for } \omega_{CB}=0\ , \tag{4.2}$$

where

$$\gamma=\gamma_{CA}=\gamma_{CB}=\tfrac{1}{2}\gamma_3+\tfrac{1}{4}\gamma_2\ . \tag{4.3}$$

A similar expression with $A \Longleftrightarrow B$, $\alpha_1 \Longleftrightarrow -\alpha_1$ gives $\tilde{\rho}_{32}(t)$ at $\omega_{CA}=0$. We now wish to examine Eq. (4.2) for two sets of initial conditions, one in which $\tilde{\rho}_{BB}(0)=1$ and one in which $\tilde{\rho}_{BB}(0)=\tilde{\rho}_{AA}(0)=\tilde{\rho}_{AB}(0)=\tilde{\rho}_{BA}(0)=\frac{1}{2}$.

1. *Preparation in a single dressed state $\tilde{\rho}_{BB}(0)=1$*

In this limit, for which $\tilde{\rho}_{AA}(0)=\tilde{\rho}_{AB}(0)=0$, Eq. (4.2) reduces to

$$\tilde{\rho}_{32}(t)\simeq\begin{cases}-\dfrac{i\alpha_2}{4}\left[\dfrac{1-e^{-\gamma t}}{\gamma}+\dfrac{e^{-(1/2)\gamma_2 t}-e^{-\gamma t}}{\gamma-\frac{1}{2}\gamma_2}+\dfrac{1-e^{-(1/2)\gamma_2 t}}{\gamma+2i\alpha_1}\right] & (\omega_{CB}=0)\\ -\dfrac{i\alpha_2}{4}\left[\dfrac{1+e^{-(1/2)\gamma_2 t}-2e^{-(\gamma-2i\alpha_1)t}}{\gamma-2i\alpha_1}+\dfrac{1-e^{-\gamma t}}{\gamma}-\dfrac{e^{-(1/2)\gamma_2 t}-e^{-\gamma t}}{\gamma-\frac{1}{2}\gamma_2}\right] & (\omega_{CA}=0)\ .\end{cases} \tag{4.4}$$

Recall that $\gamma=\frac{1}{2}\gamma_3+\frac{1}{4}\gamma_2$. If γt is much less than unity, we see that the peak at $\omega_{CB}=0$ builds up as $\alpha_2 t/2$ while that at $\omega_{CA}=0$ builds up, on average, as $\frac{1}{2}[(\gamma_2/4)t][(\alpha_2/2)t] \ll \alpha_2 t$. There is also an oscillatory component at $\omega_{CA}=0$ which varies inversely with α_1. This result is entirely consistent with the discussion in Sec. II and can be understood with the aid of Fig. 3. When one starts the system in dressed state B, state C is resonant with state B if $\omega_{CB}=0$ and a transition amplitude $\alpha_B t/\sqrt{2}=\frac{1}{2}\alpha_2 t$ is obtained. However, if $\omega_{CA}=0$, there are two pathways for excitation of state C. First, there is a stepwise excitation in which the system goes from state B to A (with amplitude $=\gamma_2 t/4$ for $\gamma t \ll 1$) and then from A to C (with amplitude $\frac{1}{2}\alpha_2 t$), giving an overall contribution to the total amplitude for the ω_{CA} resonance of $\frac{1}{2}(\frac{1}{4}\gamma_2 t)(\frac{1}{2}\alpha_2 t)$ at early times. Second, there is a direct transition between states B and C, giving rise to an oscillatory component at the ω_{CA} resonance. At early times, its contributions to the ω_{CA} resonance can be relatively important (the atom acts in some sense as an undamped oscillator), but for longer times ($\gamma_2 t \gtrsim 1$, $\gamma_3 t \gtrsim 1$) its relative contribution is of order γ/α_1. Thus, we expect the buildup of the $\omega_{CA}=0$ resonance peak to be suppressed relative to that of the $\omega_{CB}=0$ peak if we start in dressed state B, and we expect to see some oscillations in the ω_{CA} resonance peak buildup. Note that these oscillations damp out in a time of order $\min(\gamma_2^{-1},\gamma_3^{-1})$.

The features described above are easily seen in Fig. 4. These figures display buildup at the absorption resonance peaks $[-\mathrm{Im}\tilde{\rho}_{32}(t)]$ for the initial condition $\tilde{\rho}_{BB}(0)=1$ for $|\chi|/\gamma_3=2\alpha_1/\gamma_3=20$, $\gamma_2/\gamma_3=1.5$ [Fig. 4(a)] and $|\chi|/\gamma_3=2\alpha_1/\gamma_3=2$, $\gamma_2/\gamma_3=0.05$ [Fig. 4(b)]. The ω_{CB} resonance builds up more rapidly than the ω_{CA} resonance. Oscillations are seen in the ω_{CA} resonance which damp out more rapidly in Fig. 4(b) than Fig. 4(a). By using Eqs. (3.28) and (4.4) one can calculate $\tilde{\rho}_{33}(t)$. Graphs of $\tilde{\rho}_{33}(t)$ for the same choice of parameters as in Fig. 4 are shown in Figs. 5(a) and 5(b). The population builds up more rapidly for the ω_{CB} resonance than the ω_{CA} resonance when $\tilde{\rho}_{BB}(0)=1$. In calculating $\tilde{\rho}_{33}(t)$ one finds that the oscillatory structures seen in Fig. 4 are smoothed out on a time scale γ_3^{-1}.

2. *Preparation with $\tilde{\rho}_{AA}(0)=\tilde{\rho}_{BB}(0)=\tilde{\rho}_{AB}(0)=\tilde{\rho}_{BA}(0)=\frac{1}{2}$*

This limit corresponds to an initial condition in which the atom is in bare state 1 at $t=0$, i.e., $\tilde{\rho}_{11}(0)=1$. As discussed in Sec. II, we should now expect to see important oscillations (nutation) in the transient buildup of the resonance peaks. The nutation can be attributed to the fact that $\tilde{\rho}_{AB}(0)\neq 0$ which, in turn, can be associated with the fact that the Bloch vector $\mathbf{B}_{12}$ and the $\mathbf{\Omega}_B$ vector are no longer parallel at $t=0$ as they were when the atoms were prepared in a single dressed state.

For the initial conditions $\tilde{\rho}_{\mu\nu}(0)=\frac{1}{2}$ ($\mu,\nu=A$ or B), and for $\Delta_{21}=0$ ($\theta=\pi/4$), it follows from Eq. (4.2) that

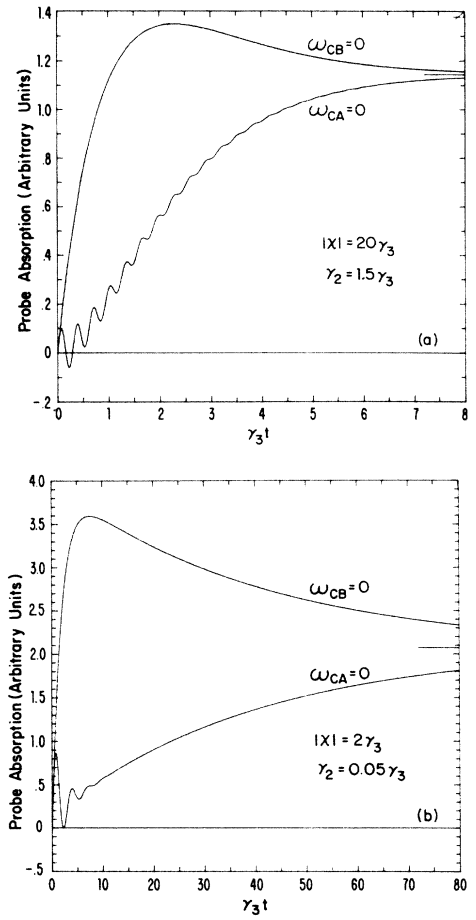

FIG. 4. The transient probe absorption $[-\mathrm{Im}\tilde{\rho}_{32}(t)]$ at the two resonance peaks $\omega_{CB}=0$ ($\Delta_{32}=|\chi|/2$) and $\omega_{CA}=0$ ($\Delta_{32}=-|\chi|/2$) as a function of $\gamma_3 t$ when a strong pump (dressing) field is exactly on resonance with the 1-2 transition ($\Delta_{21}=0$), the atom is initially in a single dressed state $\tilde{\rho}_{BB}(0)=1$, and (a) $|\chi|=2\alpha_1=20\gamma_3$, $\gamma_2=1.5\gamma_3$, (b) $|\chi|=2\alpha_1=2\gamma_3$, $\gamma_2=0.05\gamma_3$. The short bars on the right-hand side indicate the steady-state value which is independent of initial conditions and is the same for the two peaks. The choice of parameters of (a) [(b)] apply to all figures (a) [(b)] in Figs. 4–11.

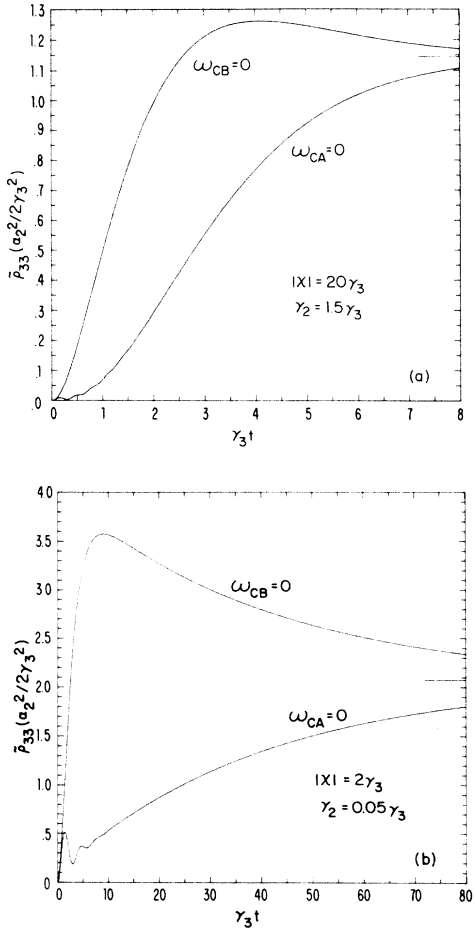

FIG. 5. The transient behavior of the upper state population $\tilde{\rho}_{33}(t)$ at the two resonance peaks $\omega_{CB}=0$ and $\omega_{CA}=0$ for the same situation as in Fig. 4. The short bar on the right-hand side indicates a steady-state value which is independent of initial atomic conditions and is the same for the two peaks. The population is measured in units of $\alpha_2^2/(2\gamma_3^2)$ which is always assumed to be much less than unity.

$$\tilde{\rho}_{32}(t)=-\frac{i\alpha_2}{4}\left[\frac{1-e^{-(\gamma+2i\alpha_1)t}}{\gamma+2i\alpha_1}+\frac{1-e^{-\gamma t}}{\gamma}\right]+\frac{i\alpha_2}{4}\left[\frac{e^{-2i\alpha_1 t}(e^{-(3/4)\gamma_2 t}-e^{-\gamma t})}{\gamma-\frac{3}{4}\gamma_2}+\frac{e^{-[(3/4)\gamma_2-2i\alpha_1]t}-e^{-\gamma t}}{\gamma-\frac{3}{4}\gamma_2+2i\alpha_1}\right],\quad \text{for } \omega_{CB}=0\,. \tag{4.5}$$

The probe absorption, proportional to $-\mathrm{Im}\tilde{\rho}_{32}(t)$, and the upper state population $\tilde{\rho}_{33}(t)$ are now symmetric about $\Delta_{32}=0$ owing to the inherent symmetry of the initial conditions, so that it is sufficient to consider the $\omega_{CB}=0$ resonance only. If $\gamma t \ll 1$, the probe absorption builds up as $\frac{1}{4}\alpha_2 t[1-\cos(2\alpha_1 t)]$.[29] For all t, the buildup is characterized by nutation oscillations of frequency $2\alpha_1$.

In Figs. 6 and 7, we graph $-\mathrm{Im}\tilde{\rho}_{32}(t)$ and $\tilde{\rho}_{33}(t)$, respectively, for the same field and decay parameters as in Figs. 4 and 5, but with the new initial condition $\tilde{\rho}_{11}(0)=1$. Oscillations are seen in the probe absorption buildup at the resonance peaks. In calculating $\tilde{\rho}_{33}(t)$, these oscillations are smoothed over a time γ_3^{-1}. Thus, in Fig. 7(a), in which $|\chi|=2\alpha_1=20\gamma_3$, the population oscillations are greatly reduced from those in the probe absorption [Fig. 6(a)]; however, in Fig. 7(b), in which $|\chi|=2\alpha_1=2\gamma_3$, smoothing does not result in such a dramatic reduction in the oscillation amplitude.

B. Transient probe spectra

The full transient probe-absorption spectra and upper state population are given in Figs. 8–11 corresponding to the parameters chosen in Figs. 4–7, respectively. These

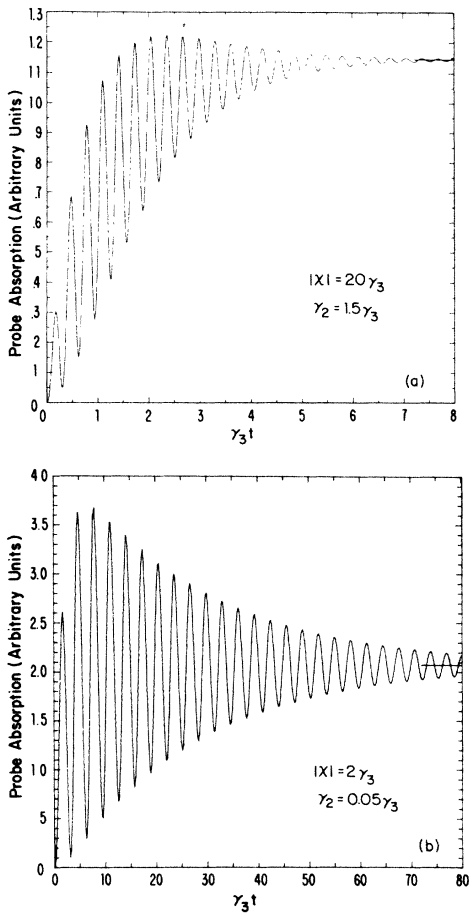

FIG. 6. Same as in Fig. 4 except that the initial conditions are now $\tilde{\rho}_{AA}(0)=\tilde{\rho}_{BB}(0)=\tilde{\rho}_{BA}(0)=\frac{1}{2}$, i.e., $\tilde{\rho}_{11}(0)=1$. The probe absorption is the same at the resonance peaks $\omega_{CB}=0$ and $\omega_{CA}=0$ owing to the resonant dressing field and the symmetry in the initial conditions in the DAP.

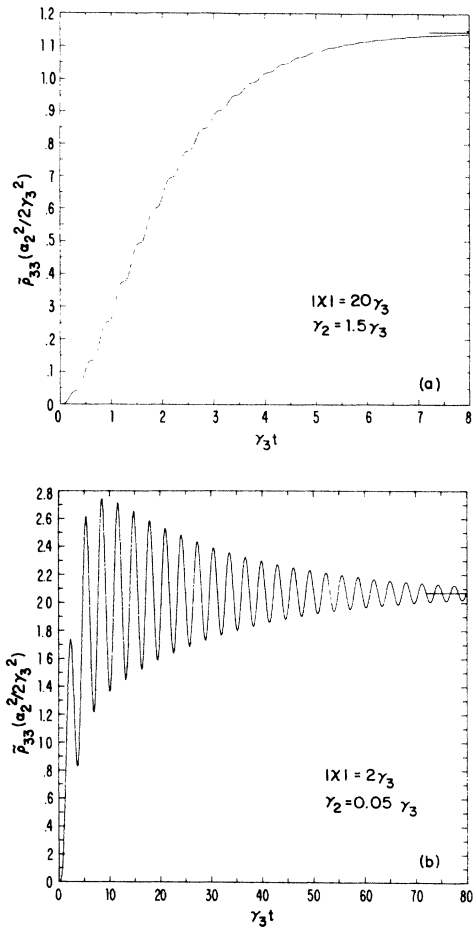

FIG. 7. Same as in Fig. 5 except that the initial conditions are now $\tilde{\rho}_{AA}(0)=\tilde{\rho}_{BB}(0)=\tilde{\rho}_{BA}(0)=\frac{1}{2}$, i.e., $\tilde{\rho}_{11}(0)=1$. The $\tilde{\rho}_{33}(t)$ are the same at the resonance peaks $\omega_{CB}=0$ and $\omega_{CA}=0$.

curves have been calculated from Eqs. (3.26)–(3.28). While these figures are fairly self-explanatory, the following three features may be noted.

(1) At very early times ($2\alpha_1 t \ll 1$), the spectra are independent of detuning Δ_{32} for $|\Delta_{32}| \lesssim 2\alpha_1$; this feature is associated with the fact that the probe switching is assumed to occur on a time scale much less than α_1^{-1}.

(2) Spectra with $\tilde{\rho}_{11}(0)=1$ are symmetric about $\Delta_{32}=0$ for the assumed detuning $\Delta_{21}=0$.

(3) Oscillations in Figs. 8(b) and 9(b) are totally damped for all detunings, once $\gamma_3 t \gg 1$; this is linked to the fact that $\alpha_1 \simeq \gamma_3 \gg \gamma_2$.

Figures 8–11 clearly show that, for atoms prepared in a single dressed state, the buildup of one of the resonance peaks is suppressed and nutation oscillations are all but eliminated.

V. INITIAL CONDITIONS FOR DRESSED STATES

The atoms are prepared in their initial state during the period $-\infty < t \leq 0$. This preparation can be done by using cw or transient methods. At $t=0$, the initial dressed-state density-matrix elements are related to the bare-state ones by

$$\tilde{\rho}_{AA}=\tfrac{1}{2}-\tfrac{1}{2}u\sin(2\theta)-\tfrac{1}{2}w\cos(2\theta)\ , \tag{5.1a}$$

$$\tilde{\rho}_{BB}=\tfrac{1}{2}+\tfrac{1}{2}u\sin(2\theta)+\tfrac{1}{2}w\cos(2\theta)\ , \tag{5.1b}$$

$$\tilde{\rho}_{BA}=\tfrac{1}{2}u\cos(2\theta)-\tfrac{1}{2}iv-\tfrac{1}{2}w\sin(2\theta)\ , \tag{5.1c}$$

$$\tilde{\rho}_{AB}=\tilde{\rho}_{BA}^{*}\ , \tag{5.1d}$$

where u, v, and w are given by Eq. (2.2) and θ is determined by Eq. (3.3). It is important to note that our Bloch equations as well as Eqs. (5.1) are defined relative to the phase of the dressing field present for $t>0$.[25]

By proper state preparation, any set of initial conditions can be achieved. For example, assuming a resonant dressing field ($\theta=\pi/4$), if the (1) atoms are in bare state 1 ($\tilde{\rho}_{11}=1$, all other $\tilde{\rho}_{ij}=0$) (in this case, no active preparation is necessary),

$$\tilde{\rho}_{AA}(0)=\tilde{\rho}_{BB}(0)=\tilde{\rho}_{AB}(0)=\tilde{\rho}_{BA}(0)=\tfrac{1}{2}\ ; \tag{5.2}$$

(2) atoms are prepared using a $\pi/2$ pulse by a field having the same phase as the dressing field ($u=0$, $v=1$, $w=0$),

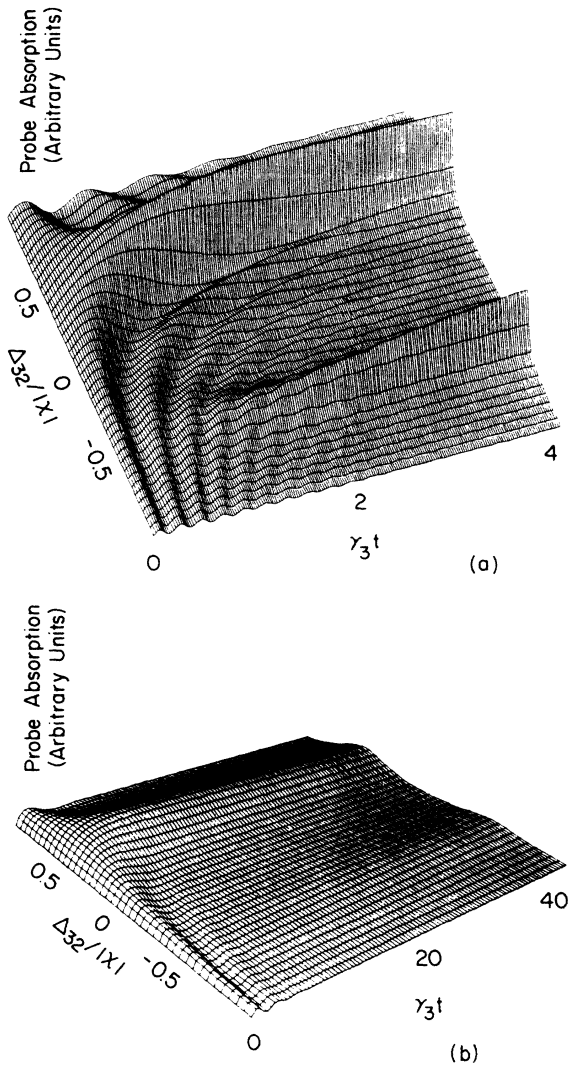

FIG. 8. The transient probe absorption ($-\mathrm{Im}\tilde{\rho}_{32}$) spectra as a function of both probe detuning ($\Delta_{32}/|\chi|$) and time ($\gamma_3 t$) for the same situation and initial conditions as in Fig. 4, namely, $\Delta_{21}=0$, $\tilde{\rho}_{BB}(0)=1$, and (a) $|\chi|=2\alpha_1=20\gamma_3$, $\gamma_2=1.5\gamma_3$, (b) $|\chi|=2\alpha_1=2\gamma_3$, $\gamma_2=0.05\gamma_3$. The transient probe response is plotted up to only half of the time range in Figs. 4–7 and, consequently, has not yet arrived at the steady-state spectra which are independent of initial conditions and are given in Fig. 2.

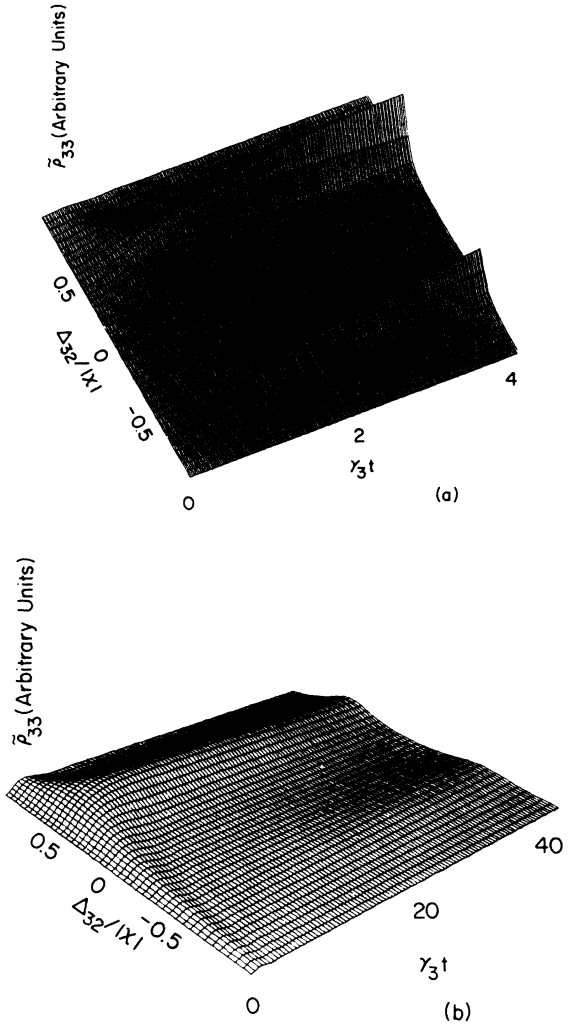

FIG. 9. Same as in Fig. 8 except that it is drawn for the upper level population $\tilde{\rho}_{33}(t)$. The steady-state spectra are also those in Fig. 2. The transient response at the two peaks $\Delta_{32}=\pm|\chi|/2$ are also given in Fig. 5.

$$\tilde{\rho}_{AA}(0)=\tilde{\rho}_{BB}(0)=\tfrac{1}{2},\quad \tilde{\rho}_{AB}(0)=-\tilde{\rho}_{BA}(0)=i/2\ ; \tag{5.3}$$

(3) atoms are prepared using a $\pi/2$ pulse by a field that is $\pm\pi/2$ out of phase with the dressing field ($u=\pm1$, $v=0$, $w=0$),

$$\tilde{\rho}_{BB}(0)=1,\ \tilde{\rho}_{AA}(0)=\tilde{\rho}_{AB}(0)=\tilde{\rho}_{BA}(0)=0\ , \tag{5.4a}$$

or

$$\tilde{\rho}_{AA}(0)=1,\ \tilde{\rho}_{BB}(0)=\tilde{\rho}_{AB}(0)=\tilde{\rho}_{BA}(0)=0\ . \tag{5.4b}$$

As has been pointed out recently,[7] example (3) produces atoms in pure dressed states. In examples (2) and (3) above, relaxation processes during the application of the $\pi/2$ pulses were neglected, and the preparatory pulses were assumed to terminate at the time of application of the dressing fields.

Generally, for a nonresonant dressing field ($\Delta_{21}\neq0$), one also can prepare a pure dressed state by the phase-switching method. One knows from Eqs. (5.1) that the pure dressed state $|B\rangle$ ($|A\rangle$) is produced when the Bloch vector $\mathbf{B}_{12}$ is parallel (antiparallel) to the driving vector $\mathbf{\Omega}_B=(\omega_{BA}\sin2\theta,0,\omega_{BA}\cos2\theta)$. A schematic diagram is given in Fig. 12 showing how to align the Bloch vector $\mathbf{B}_{12}$ along the driving vector $\mathbf{\Omega}_B$. We can show that, at first, a field is applied to rotate $\mathbf{B}_{12}$ from its original downward position ($\tilde{\rho}_{11}=1$) by an angle

$$\psi_1=\arccos\left[1-\frac{1}{2\cos^2[\pi/4-|(\pi/4)-\theta|]}\right]$$
$$=\arccos\left[\frac{1}{[1+(2\alpha_1/\Delta_{21})^2]^{1/2}+1}\right] \tag{5.5}$$

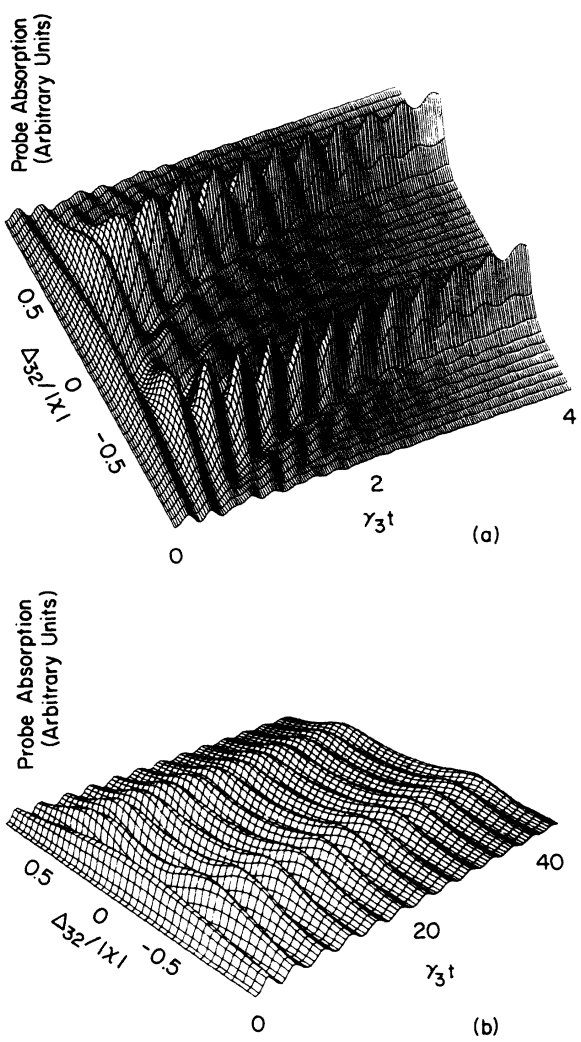

FIG. 10. Same as in Fig. 8 except that the initial conditions are now $\tilde{\rho}_{AA}(0)=\tilde{\rho}_{BA}(0)=\frac{1}{2}$. The spectra are symmetric about zero probe detuning ($\Delta_{32}=0$) and the transient behavior at the peaks are also given in Fig. 6.

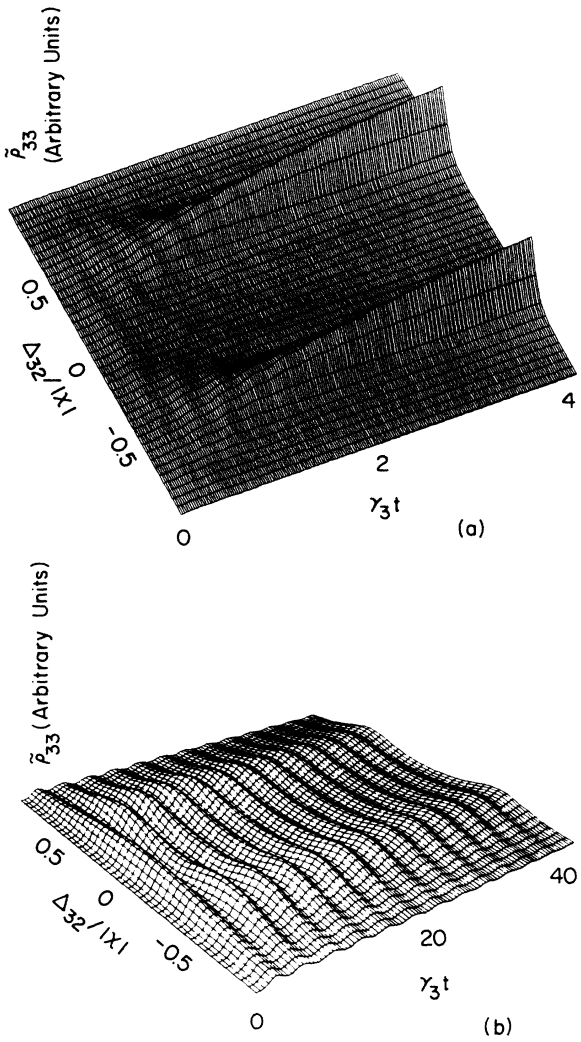

FIG. 11. Same as in Fig. 9 except that the initial conditions are now $\tilde{\rho}_{AA}(0)=\tilde{\rho}_{BB}(0)=\tilde{\rho}_{BA}(0)=\frac{1}{2}$ and the transient response at the peaks are given in Fig. 7. The spectra are symmetric about zero probe detuning.

(or angle $2\pi-\psi_1$) to position P (or Q) such that $-\mathbf{B}_{12}$ (when $\Delta_{21}>0$) or $\mathbf{B}_{12}$(when $\Delta_{21}<0$) aligns along one of two intersection lines of two cones formed by the rotation of $\pm\hat{w}$ about $\mathbf{\Omega}_B$ and that of $\mathbf{\Omega}_B$ about $\hat{w}$, respectively. Then, $\mathbf{\Omega}_B$ should be rotated about $-\hat{w}$ (or $+\hat{w}$) with angle

$$\psi_2=\arctan\frac{[1+2\sin|(\pi/2)-2\theta|]^{1/2}}{|\cos 2\theta|}$$
$$=\arctan\left\{\left[1+\left[\frac{2\alpha_1}{\Delta_{21}}\right]^2\right]^{1/2}\times\left\{\left[1+\left[\frac{2\alpha_1}{\Delta_{21}}\right]^2\right]^{1/2}+2\right\}\right\}^{1/2} \quad (5.6)$$

to coincide with the rotated $\mathbf{B}_{12}$ vector. The first step can be performed by a step-function preparation dressing field of duration $\psi_1(\Delta_{21}^2+4\alpha_1^2)^{-1/2}$ and the second step should be carried out very quickly by changing the phase of the dressing field by ψ_2. The atomic state preparation must be carried out in a period much shorter than γ_2^{-1}.

One can also produce the atoms in a pure dressed state by adiabatically turning on the dressing field in the period $-\infty<t\leq 0$.[8,30] In this method, adiabaticity is achieved by using a value $\sin 2\theta\ll 1$ (i.e., a large detuning Δ_{21}) to insure that the Bloch and $\mathbf{\Omega}_B$ vectors remain parallel—this leads to probe absorption signals that are smaller by a factor $\sin^2 2\theta$ than those produced by the phase-switching method. Adiabatic following can also be achieved by starting with an off-resonant laser field and slowly sweeping its frequency into resonance. This method could be used to produce atoms in a single dressed state which would produce probe-absorption spectra comparable in strength to those produced by the phase-switching method.

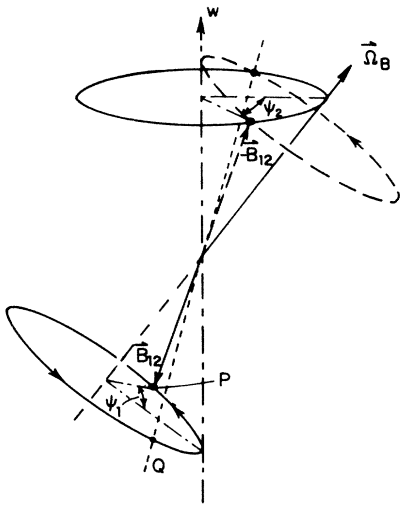

FIG. 12. Aligning the Bloch vector $\mathbf{B}_{12}$ along the driving vector $\mathbf{\Omega}_B$ in a nonresonant dressing field $\Delta_{21}>0$ case. At first, a step-function dressing field of duration $\psi_1(\Delta_{21}^2+\chi^2)^{-1/2}$ rotates the Bloch vector $\mathbf{B}_{12}$ from its original downward $[w(0)=-1]$ position to position P. Then, the driving vector $\mathbf{\Omega}_B$ is rotated to coincide with rotated $-\mathbf{B}_{12}$ by decreasing the phase of dressing field very quickly by ψ_2. After this the Bloch vector $\mathbf{B}$ is antiparallel with $\mathbf{\Omega}_B$.

VI. CONCLUSION

The transient response of atoms in an atomic beam to a step-function weak probe and strong pump field has been described. The probe-absorption spectral response was found to be a sensitive function of the initial conditions of the dressed atoms. In the case of a resonant pump field and equally populated dressed states at the time the probe field is turned on, the probe spectrum is double peaked and symmetric, and the resonance peaks exhibit oscillations as they evolve toward their steady-state values. In contrast, if the atoms are initially prepared into a single dressed state (using the means described), the probe spectrum is initially asymmetric and the resonance peaks do not oscillate appreciably as they approach the same steady-state values. Our calculations demonstrate the qualitatively new behavior observable in transient studies where initial atomic conditions can be controlled. Although we only considered an upward-cascade closed system in this paper, oscillation disappearance and the suppression of one peak can also occur in various other three-level configurations with or without the presence of incoherent pumping. In closing, we note that the transient studies of resonance fluorescence of a two-level system should also be interesting, since atoms prepared in a pure dressed state should initially display only a double-peaked spectrum.

ACKNOWLEDGMENTS

This research is supported, in part, by the U.S. Office of Naval Research, the U.S. Joint Services Electronics Program, and the National Science Foundation under Grants No. PHY-84-15781 and No. PHY-85-04260. One of us (A.G.Y.) acknowledges financial support from the U.S. Army.

APPENDIX A

The elements $R_{\xi\sigma,\mu\nu}$ represent the effects of spontaneous emission or collision relaxation in the DAP. The nonvanishing $R_{\xi\sigma,\mu\nu}$ are[6]

$$R_{AA,AA}=-\Gamma_1\cos^2\theta-\Gamma_2\sin^2\theta -\tfrac{1}{4}(\eta-\Gamma_{12}-\Gamma_{21})\sin^2(2\theta)\ , \tag{A1a}$$

$$R_{AA,BB}=\tfrac{1}{4}\eta\sin^2(2\theta)+\Gamma_{12}\sin^4\theta+\Gamma_{21}\cos^4\theta\ , \tag{A1b}$$

$$R_{AA,CC}=\Gamma_{32}\sin^2\theta\ , \tag{A1c}$$

$$R_{AA,AB}=R_{AA,BA} =\tfrac{1}{4}\sin2\theta[\Gamma_2-\Gamma_1+\eta\cos(2\theta) -2\Gamma_{21}\cos^2\theta+2\Gamma_{12}\sin^2\theta]\ , \tag{A1d}$$

$$R_{BB,AA}=\tfrac{1}{4}\eta\sin^2(2\theta)+\Gamma_{12}\cos^4\theta+\Gamma_{21}\sin^4\theta\ , \tag{A2a}$$

$$R_{BB,BB}=-\Gamma_1\sin^2\theta-\Gamma_2\cos^2\theta -\tfrac{1}{4}(\eta-\Gamma_{12}-\Gamma_{21})\sin^2(2\theta)\ , \tag{A2b}$$

$$R_{BB,CC}=\Gamma_{32}\cos^2\theta\ , \tag{A2c}$$

$$R_{BB,AB}=R_{BB,BA} =\tfrac{1}{4}\sin2\theta[\Gamma_2-\Gamma_1-\eta\cos(2\theta) +2\Gamma_{12}\cos^2\theta-2\Gamma_{21}\sin^2\theta]\ , \tag{A2d}$$

$$R_{CC,CC}=-\Gamma_3\ , \tag{A3a}$$

$$R_{CC,AA}=\Gamma_{23}\sin^2\theta\ , \tag{A3b}$$

$$R_{CC,BB}=\Gamma_{23}\cos^2\theta\ , \tag{A3c}$$

$$R_{CC,AB}=R_{CC,BA}=-\tfrac{1}{2}\Gamma_{23}\sin^2\theta\ , \tag{A3d}$$

$$R_{BA,AA}=\tfrac{1}{4}\sin(2\theta)[\Gamma_2-\Gamma_1+\eta\cos(2\theta) +2\Gamma_{21}\sin^2\theta-2\Gamma_{12}\cos^2\theta]\ , \tag{A4a}$$

$$R_{BA,BB}=\tfrac{1}{4}\sin2\theta[\Gamma_2-\Gamma_1-\eta\cos(2\theta) +2\Gamma_{21}\cos^2\theta-2\Gamma_{12}\sin^2\theta]\ , \tag{A4b}$$

$$R_{BA,CC}=-\tfrac{1}{2}\Gamma_{32}\sin(2\theta)\ , \tag{A4c}$$

$$R_{BA,AB}=\tfrac{1}{4}(\eta-\Gamma_{12}-\Gamma_{21})\sin^2(2\theta)\ , \tag{A4d}$$

with the remaining elements given by the symmetry property

$$R_{\xi\sigma,\mu\nu}=R_{\sigma\xi,\nu\mu}\ . \tag{A5}$$

APPENDIX B

By substituting Eqs. (3.27) and (3.26) into Eq. (3.28) and using Eq. (3.11), one obtains the general expression of $\tilde{\rho}_{33}(t)$ as

$$\begin{aligned}\tilde{\rho}_{33}(t)=&\frac{2\alpha_2^2(1-e^{-\gamma_3 t})}{\gamma_3\Gamma_p}\left[\frac{a\gamma_{CB}\cos^2\theta}{\gamma_{CB}^2+\omega_{CB}^2}+\frac{b\gamma_{CA}\sin^2\theta}{\gamma_{CA}^2+\omega_{CA}^2}\right]\\&+\frac{2\alpha_2^2[b\tilde{\rho}_{BB}(0)-a\tilde{\rho}_{AA}(0)](e^{-\Gamma_p t}-e^{-\gamma_3 t})}{\Gamma_p(\gamma_3-\Gamma_p)}\left[\frac{(\gamma_{CB}-\Gamma_p)\cos^2\theta}{(\gamma_{CB}-\Gamma_p)^2+\omega_{CB}^2}-\frac{(\gamma_{CA}-\Gamma_p)\sin^2\theta}{(\gamma_{CA}-\Gamma_p)^2+\omega_{CA}^2}\right]\\&+\frac{2\alpha_2^2[b\tilde{\rho}_{BB}(0)-a\tilde{\rho}_{AA}(0)]}{\Gamma_p}\mathrm{Re}\left[\frac{(e^{-(\gamma_{CB}+i\omega_{CB})t}-e^{-\gamma_3 t})\cos^2\theta}{(\gamma_{CB}+i\omega_{CB}-\Gamma_p)(\gamma_{CB}+i\omega_{CB}-\gamma_3)}\right.\\&\qquad\left.-\frac{(e^{-(\gamma_{CA}+i\omega_{CA})t}-e^{-\gamma_3 t})\sin^2\theta}{(\gamma_{CA}+i\omega_{CA}-\Gamma_p)(\gamma_{CA}+i\omega_{CA}-\gamma_3)}\right]\\&+\frac{2\alpha_2^2}{\Gamma_p}\mathrm{Re}\left[\frac{a(e^{-(\gamma_{CB}+i\omega_{CB})t}-e^{-\gamma_3 t})\cos^2\theta}{(\gamma_{CB}+i\omega_{CB})(\gamma_{CB}+i\omega_{CB}-\gamma_3)}+\frac{b(e^{-(\gamma_{CA}+i\omega_{CA})t}-e^{-\gamma_3 t})\sin^2\theta}{(\gamma_{CA}+i\omega_{CA})(\gamma_{CA}+i\omega_{CA}-\gamma_3)}\right]\\&+\alpha_2^2\sin(2\theta)\mathrm{Re}\left\{\tilde{\rho}_{BA}(0)\left[\frac{e^{-(\gamma_{BA}+i\omega_{BA})t}-e^{-\gamma_3 t}}{\gamma_{BA}+i\omega_{BA}-\gamma_3}\left[\frac{1}{\gamma_{CA}-\gamma_{BA}+i\omega_{CB}}+\frac{1}{\gamma_{CB}-\gamma_{BA}-i\omega_{CA}}\right]\right.\right.\\&\qquad-\frac{e^{-(\gamma_{CA}+i\omega_{CA})t}-e^{-\gamma_3 t}}{(\gamma_{CA}-\gamma_{BA}+i\omega_{CB})(\gamma_{CA}-\gamma_3-i\omega_{CA})}\\&\qquad\left.\left.-\frac{e^{-(\gamma_{CB}-i\omega_{CB})t}-e^{-\gamma_3 t}}{(\gamma_{CB}-\gamma_{BA}-i\omega_{CA})(\gamma_{CB}-\gamma_3-i\omega_{CB})}\right]\right\}.\end{aligned}\tag{B1}$$

[1]B. R. Mollow, Phys. Rev. **188**, 1969 (1969); F. Schuda, C. R. Stroud, Jr., and M. Hercher, J. Phys. B **7**, L198 (1974); H. Walther, in *Laser Spectroscopy II*, edited by S. Haroche, J. C. Pebay-Peyroula, T. W. Hansch, and S. H. Harris (Springer-Verlag, Berlin, 1975), p. 358; F. Y. Wu, R. E. Grove, and S. Ezekiel, Phys. Rev. Lett. **35**, 1426 (1975); R. E. Grove, F. Y. Wu, and S. Ezekiel, Phys. Rev. A **15**, 227 (1977); C. Cohen-Tannoudji and S. Reynaud, in *Multiphoton Processes*, edited by J. H. Eberly and P. Lambropoulos (Wiley, New York, 1978).

[2]B. R. Mollow, Phys. Rev. A **5**, 2217 (1972); F. Y. Wu, S. Ezekiel, M. Ducloy, and B. R. Mollow, Phys. Rev. Lett. **38**, 1077 (1977); C. Cohen-Tannoudji and S. Reynaud, J. Phys. B **10**, 345 (1977).

[3]S. H. Autler and C. H. Townes, Phys. Rev. **100**, 703 (1955); A. Schabert, R. Keil, and P. E. Toschek, Appl. Phys. **6**, 181 (1975); J. L. Picqué and J. Pinard, J. Phys. B **9**, L77 (1976); H. R. Gray and C. R. Stroud, Jr., Opt. Commun. **25**, 359 (1978); P. R. Hermmer, B. W. Peuse, F. Y. Wu, J. E. Thomas, and S. Ezekiel, Opt. Lett. **6**, 531 (1981).

[4]See, for example, C. Cohen-Tannoudji, in *Frontiers in Laser Spectroscopy*, edited by R. Balian, S. Haroche, and S. Liberman (North-Holland, Amsterdam, 1977).

[5]E. Courtens and A. Szoke, Phys. Rev. A **15**, 1588 (1977); D. Grischkowsky, *ibid.* **14**, 802 (1976).

[6]P. R. Berman and R. Salomaa, Phys. Rev. A **25**, 2667 (1982).

[7]Y. S. Bai, A. G. Yodh, and T. W. Mossberg, Phys. Rev. Lett. **55**, 1277 (1985).

[8]D. Grischkowsky, Phys. Rev. A **7**, 2096 (1973).

[9]D. Grischkowsky, M. M. T. Loy, and P. F. Liao, Phys. Rev. A **12**, 2514 (1975).

[10]R. G. Brewer and E. L. Hahn, Phys. Rev. A **11**, 1641 (1975).

[11]M. Sargent III and P. Horwitz, Phys. Rev. A **13**, 1962 (1976).

[12]D. P. Hodginson and J. S. Briggs, Opt. Commun. **22**, 45 (1977).

[13]J. R. Ackerhalt and B. W. Shore, Phys. Rev. A **16**, 277 (1977); B. W. Shore and J. R. Ackerhalt, *ibid.* **15**, 1640 (1977).

[14]M. Ducloy, J. R. R. Leite, and M. S. Feld, Phys. Rev. A **17**, 623 (1978); M. Ducloy and M. S. Feld, in *Laser Spectroscopy III*, edited by J. L. Hall and J. L. Carlsten (Springer, New York, 1977), p. 243; J. R. R. Leite, R. L. Sheffield, M. Ducloy, R. D. Sharma, and M. S. Feld, Phys. Rev. A **14**, 1151 (1976); M. S. Feld, in *Frontiers in Laser Spectroscopy*, edited by R. Balian, S. Haroche, and S. Liberman (North-Holland, Amsterdam, 1977), p. 203.

[15]M. P. Silverman, S. Haroche, and M. Gross, Phys. Rev. A **18**,

1507 (1978).
[16]T. W. Mossberg, R. Kachru, S. R. Hartmann, and A. M. Flusberg, Phys. Rev. A **20**, 1976 (1979), and references therein.
[17]A. Schenzle and R. G. Brewer, Phys. Rev. A **14**, 1756 (1976); Phys. Rep. **43**, 455 (1978).
[18]L. Kancheva, D. Pushkarov, and S. Rashev, J. Phys. B **14**, 573 (1981).
[19]F. Persico, Opt. Commun. **44**, 143 (1983).
[20]P. R. Berman, Opt. Commun. **52**, 225 (1984).
[21]J. H. Eberly, C. V. Kunasz, and K. Wódiewicz, J. Phys. B **13**, 217 (1980).
[22]K. I. Osman and S. Swain, Phys. Rev. A **25**, 3187 (1982).
[23]M. Ducloy, J. R. R. Leite, and M. S. Feld, Phys. Rev. A **17**, 623 (1978).
[24]See, for example, L. Allen and J. H. Eberly, *Optical Resonance and Two-Level Atoms* (Wiley, New York, 1975).
[25]Our field interaction representation is defined by

$$\tilde{\rho}_{21}=\rho_{21}\exp[i\,\mathrm{sgn}(\omega_{21})(\Omega_1 t-\mathbf{K}_1\cdot\mathbf{r}+\phi_1)]\ ,$$

$$\tilde{\rho}_{ii}=\rho_{ii}\ ,$$

as well as

$$\tilde{\rho}_{32}=\rho_{32}\exp[i\,\mathrm{sgn}(\omega_{32})(\Omega_2 t-\mathbf{K}_2\cdot\mathbf{r}+\phi_2)]\ ,$$

$$\tilde{\rho}_{31}=\rho_{31}\exp[i\,\mathrm{sgn}(\omega_{12})(\Omega_1 t-\mathbf{K}_1\cdot\mathbf{r}+\phi_1)+i\,\mathrm{sgn}(\omega_{32})(\Omega_2 t-\mathbf{K}_2\cdot\mathbf{r}+\phi_2)]$$

in anticipation of later sections. All phases are measured relative to the pump phase ϕ_1 of the field present for $t>0$. Thus, if the phase of the pump field was switched from $\phi_1+\delta$ to ϕ_1 at $t=0$, then, for $t<0$, the $\mathbf{\Omega}_B$ vector would be $(-\chi\cos\delta,-\chi\sin\delta,\Delta_{21})$.
[26]S. Hartmann and E. L. Hahn, in *Fluctuations, Relaxation and Resonance in Magnetic Systems,* edited by D. Ter Haar (Oliver and Boyd, Edinbergh, 1961); A. G. Anderson and S. R. Hartmann, Phys. Rev. **128**, 2023 (1962); S. R. Hartmann and E. L. Hahn, *ibid.* **128**, 2042 (1962).
[27]In our field-interaction representation, state $|\tilde{2}\rangle$ has an associated frequency $\tilde{\omega}_2=0$, and the frequencies associated with states $|\tilde{3}\rangle$ and $|\tilde{1}\rangle$ are $\tilde{\omega}_3=\Delta_{32}$ and $\tilde{\omega}_1=-\Delta_{21}$, respectively. In the dressed basis, $\omega_{A,B}=-\frac{1}{2}\Delta_{21}\mp\frac{1}{2}(\Delta_{21}^2+\chi^2)^{1/2}$ and $\omega_C=\Delta_{32}$.
[28]J. H. Eberly and K. Wodkiewicz, J. Opt. Soc. Am. **67**, 1252 (1977); X. Y. Huang, R. Tanas, and J. H. Eberly, Phys. Rev. A **26**, 892 (1982).
[29]Equation (4.5) is strictly valid for times $\gamma_2 t\ll\alpha_1^2 t^2$, implying also that $-\mathrm{Im}\tilde{\rho}_{32}\approx\frac{1}{4}\alpha_2 t[1-\cos(\alpha_1 t)]$ is valid only in this limit. Nevertheless, for times near $t=0$ when this inequality fails, a more complete calculation shows that this asymptotic form still remains valid for such times.
[30]D. Grischkowsky, Phys. Rev. Lett. **24**, 866 (1970); D. Grischkowsky and J. A. Armstrong, Phys. Rev. A **6**, 1566 (1972); D. Grischkowsky, E. Courtens, and J. A. Armstrong, Phys. Rev. Lett. **31**, 422 (1973).

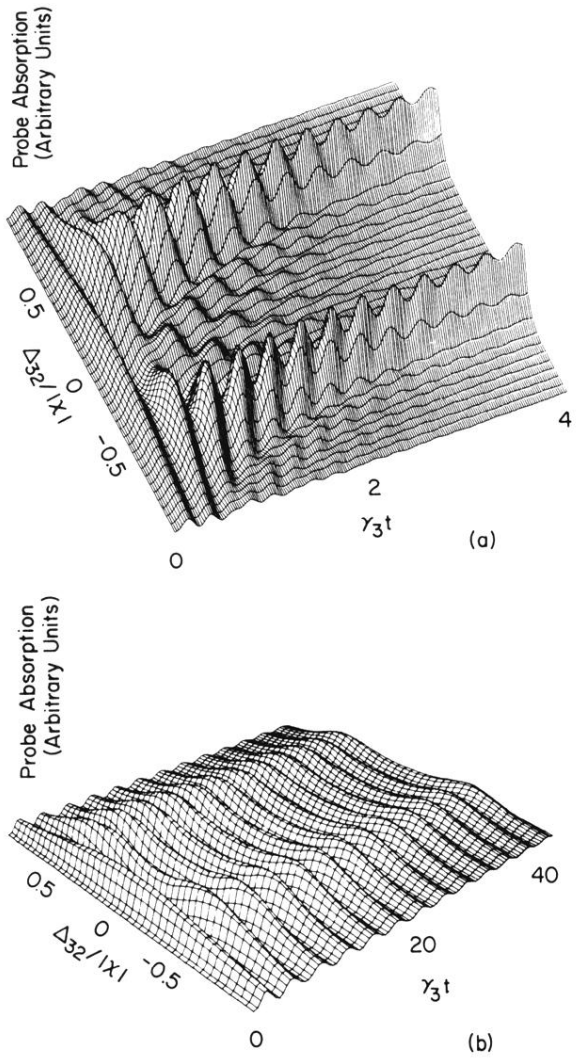

FIG. 10. Same as in Fig. 8 except that the initial conditions are now $\tilde{\rho}_{AA}(0)=\tilde{\rho}_{BA}(0)=\frac{1}{2}$. The spectra are symmetric about zero probe detuning ($\Delta_{32}=0$) and the transient behavior at the peaks are also given in Fig. 6.

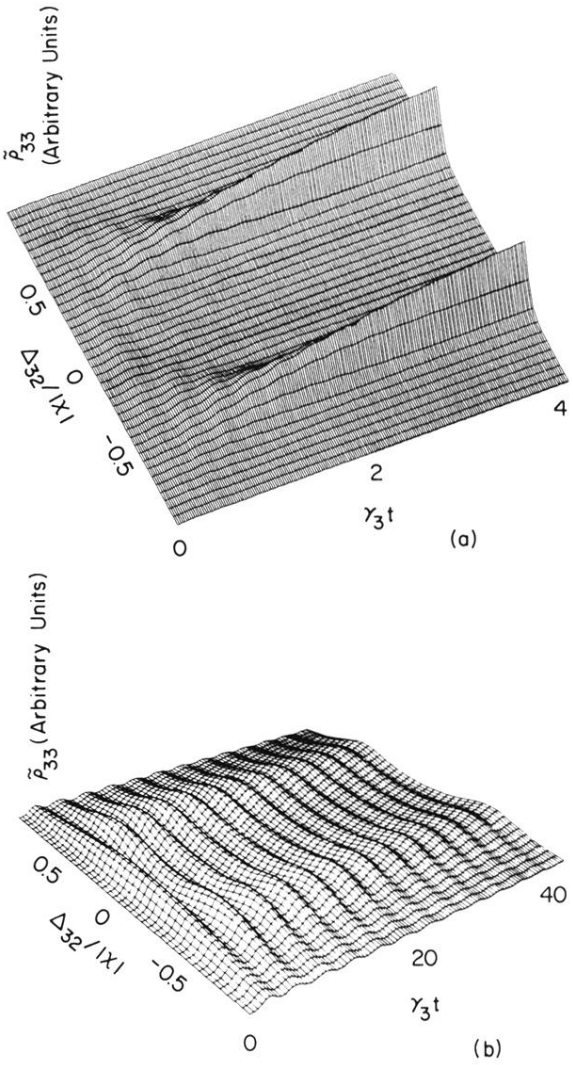

FIG. 11. Same as in Fig. 9 except that the initial conditions are now $\tilde{\rho}_{AA}(0)=\tilde{\rho}_{BB}(0)=\tilde{\rho}_{BA}(0)=\frac{1}{2}$ and the transient response at the peaks are given in Fig. 7. The spectra are symmetric about zero probe detuning.

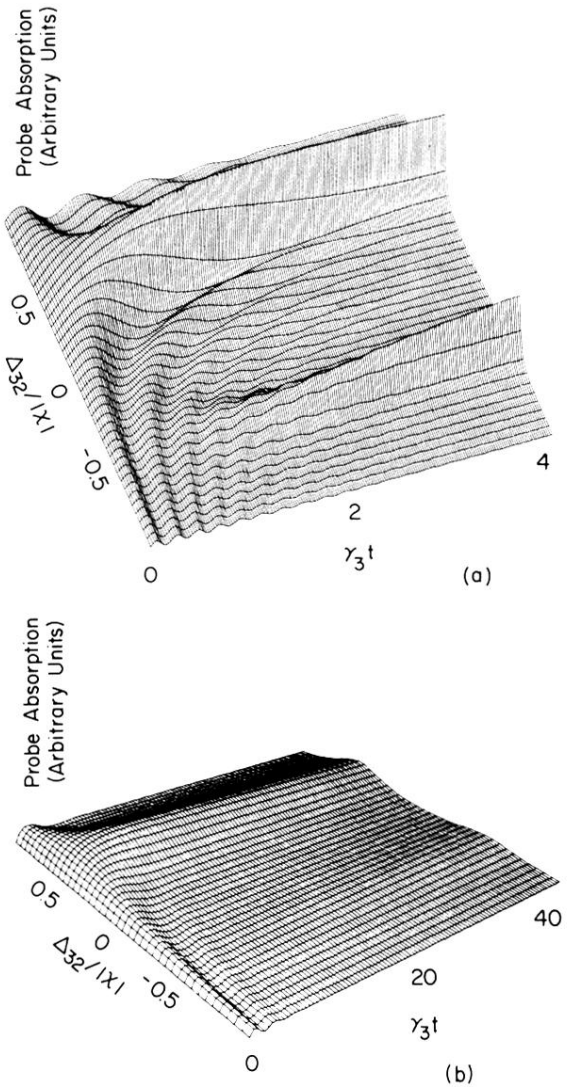

FIG. 8. The transient probe absorption ($-\mathrm{Im}\tilde{\rho}_{32}$) spectra as a function of both probe detuning ($\Delta_{32}/|\chi|$) and time ($\gamma_3 t$) for the same situation and initial conditions as in Fig. 4, namely, $\Delta_{21}=0$, $\tilde{\rho}_{BB}(0)=1$, and (a) $|\chi|=2\alpha_1=20\gamma_3$, $\gamma_2=1.5\gamma_3$, (b) $|\chi|=2\alpha_1=2\gamma_3$, $\gamma_2=0.05\gamma_3$. The transient probe response is plotted up to only half of the time range in Figs. 4–7 and, consequently, has not yet arrived at the steady-state spectra which are independent of initial conditions and are given in Fig. 2.

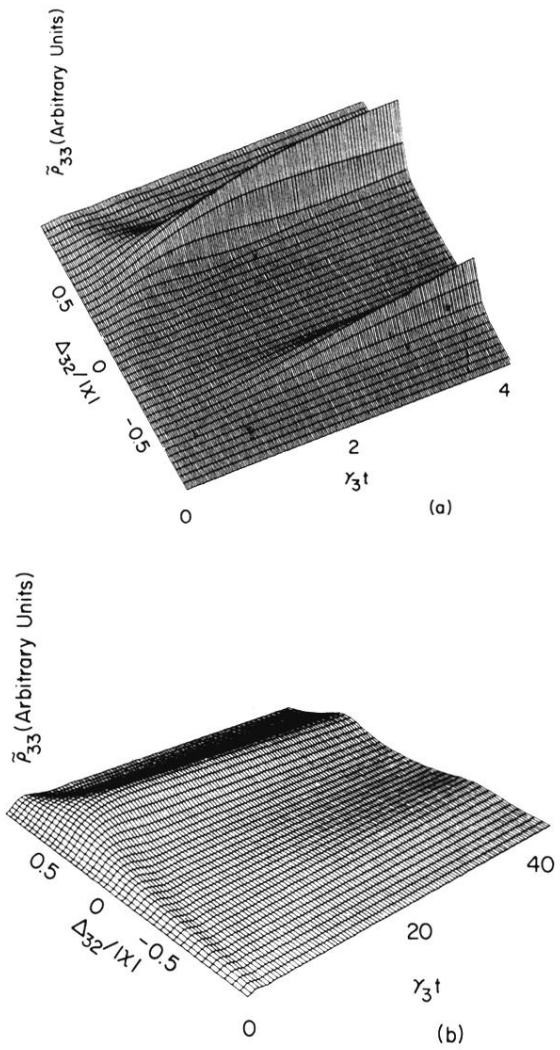

FIG. 9. Same as in Fig. 8 except that it is drawn for the upper level population $\tilde{\rho}_{33}(t)$. The steady-state spectra are also those in Fig. 2. The transient response at the two peaks $\Delta_{32} = \pm |\chi|/2$ are also given in Fig. 5.